Since January 2020 Elsevier has created a COVID-19 resource centre with free information in English and Mandarin on the novel coronavirus COVID-19. The COVID-19 resource centre is hosted on Elsevier Connect, the company's public news and information website.

Sensors & Actuators: B. Chemical 379 (2023) 133245

Contents lists available at ScienceDirect

Sensors and Actuators: B. Chemical

journal homepage: www.elsevier.com/locate/snb

A colorimetric lateral flow immunoassay based on oriented antibody immobilization for sensitive detection of SARS-CoV-2

Ae Sol Lee [a,1], Su Min Kim [a,1], Kyeong Rok Kim [a], Chulmin Park [b], Dong-Gun Lee [b,c], Hye Ryoung Heo [d], Hyung Joon Cha [e,*], Chang Sup Kim [a,f,**]

[a] Graduate School of Biochemistry, Yeungnam University, Gyeongsan 38541, Republic of Korea
[b] Vaccine Bio Research Institute, College of Medicine, Seoul St. Mary's Hospital, The Catholic University of Korea, Seoul 06591, Republic of Korea
[c] Division of Infectious Diseases, Department of Internal Medicine, College of Medicine, Seoul St. Mary's Hospital, The Catholic University of Korea, Seoul 06591, Republic of Korea
[d] Senotherapy-based Metabolic Disease Control Research Center, Yeungnam University, Gyeongsan 38541, Republic of Korea
[e] Department of Chemical Engineering, Pohang University of Science and Technology, Pohang 37673, Republic of Korea
[f] School of Chemistry and Biochemistry, Yeungnam University, Gyeongsan 38541, Republic of Korea

ARTICLE INFO

Keywords:
COVID-19
SARS-CoV-2
Orientation
Antibody
Lateral flow immunoassay
Sensitive

ABSTRACT

Severe acute respiratory syndrome coronavirus 2 (SARS-CoV-2) causes coronavirus disease 2019 (COVID-19). The high human-to-human transmission and rapid evolution of SARS-CoV-2 have resulted in a worldwide pandemic. To contain SARS-CoV-2, it is essential to efficiently control the transmission of the virus through the early diagnosis of infected individuals, including asymptomatic people. Therefore, a rapid and accurate assay is vital for the early diagnosis of SARS-CoV-2 in suspected individuals. In this study, we developed a colorimetric lateral flow immunoassay (LFIA) in which a CBP31-BC linker was used to immobilize antibodies on a cellulose membrane in an oriented manner. The developed LFIA enabled sensitive detection of cultured SARS-CoV-2 in 15 min with a detection limit of 5×10^4 copies/mL. The clinical performance of the LFIA for detecting SARS-CoV-2 was evaluated using 19 clinical samples validated by reverse transcription-polymerase chain reaction (RT—PCR). The LFIA detected all the positive and negative samples accurately, corresponding to 100% accuracy. Importantly, patient samples with low viral loads were accurately identified. Thus, the proposed method can provide a useful platform for rapid and accurate point-of-care testing of SARS-CoV-2 in infected individuals to efficiently control the COVID-19 pandemic.

1. Introduction

A novel highly infectious and pathogenic coronavirus, severe acute respiratory syndrome coronavirus 2 (SARS-CoV-2), causes coronavirus disease 2019 (COVID-19), is highly infectious and pathogenic [1]. The World Health Organization (WHO) has reported over 278 million cases globally as of 26 December 2021, including approximately 5.4 million deaths [2]. There are several drugs specific to COVID-19, but none are universally available. Therefore, rapid testing for SARS-CoV-2 is urgently needed to effectively screen COVID-19 patients in populations and manage the COVID-19 pandemic.

Reverse transcription-polymerase chain reaction (RT—PCR) is the standard method approved by the US Food and Drug Administration (FDA) for the early diagnosis of COVID-19 and has a high accuracy and a low limit of detection [3]. However, RT—PCR requires expensive reagents, specific instruments, professional technicians, and a long detection time; therefore, this technology has limitations for rapidly screening confirmed cases in a large population amid the rapid spread of SARS-CoV-2. In addition, RT—PCR is not suitable for point-of-care testing for COVID-19 diagnosis.

Lateral flow assays (LFAs) have been developed to detect SARS-CoV-2 antigens or IgG and IgM antibodies specific to SARS-CoV-2 [4–10]. LFAs may enable the screening of confirmed cases on a population scale by diagnosing COVID-19 disease quickly and inexpensively. Many LFAs

* Corresponding author.
** Corresponding author at: School of Chemistry and Biochemistry, Yeungnam University, Gyeongsan 38541, Republic of Korea.
E-mail addresses: hjcha@postech.ac.kr (H.J. Cha), cskim1409@ynu.ac.kr (C.S. Kim).
[1] These authors contributed equally to this work.

https://doi.org/10.1016/j.snb.2022.133245
Received 6 September 2022; Received in revised form 14 December 2022; Accepted 24 December 2022
Available online 26 December 2022

for COVID-19 diagnosis are in development. More than 300 LFAs have been reported to the Foundation for Innovative and New Diagnostics (FIND), of which approximately 280 are serological tests. Serological tests detect IgG and IgM in the blood of people exposed to SARS-CoV-2 [11,12]. Patients usually produce antibodies specific to SARS-CoV-2 within 19 days after symptom onset [13]; therefore, LFA antibody tests may not be useful for COVID-19 diagnosis at the early stage of infection. Antigen-detecting LFAs for SARS-CoV-2 could be used in point-of-care testing for the early screening and diagnosis of COVID-19. Commercialized antigen-detecting LFAs for SARS-CoV-2 have exhibited a sensitivity of ~30–93.9% and a specificity of 100% compared to RT—PCR [14–16]. Recently, the WHO reported interim guidelines that antigen-detecting LFAs should meet minimum performance requirements of ≥ 80% sensitivity and ≥ 97% specificity [17]. Therefore, considerable effort must be expended to improve the LFA sensitivity.

Most studies have focused on developing signal probes, whereas antibody immobilization is essential for antigen detection in LFA systems [18–21]. The orientation of immobilized antibodies significantly affects the analytical performance of an immunoassay [22–24]. Most developed antigen-detecting LFAs are based on physical adsorption of antibodies onto a nitrocellulose membrane, resulting in randomly oriented antibodies and consequently, low sensitivity [18–21]. The protein adsorption capacity of the nitrocellulose membrane makes it difficult to control the orientation of immobilized antibodies [25]. In a previous study, we developed a cellulose membrane-based sensitive lateral flow immunoassay (LFIA) using a bifunctional fusion linker, CBP31-BC, composed of cellulose-binding domains (CBDs) and antibody-binding domains [26]. Due to oriented antibody immobilization on cellulose by CBP31-BC linker, the cellulose membrane-based LFIA showed a ~10-fold higher sensitivity to prostate-specific antigens than nitrocellulose membrane-based conventional LFIAs.

In addition, cellulose paper has been widely used in many biosensors [27–29]. Recently, cellulose membrane-based LFAs have been developed for detecting SARS-CoV-2 antibodies in human serum [30]. Fusion of CBDs to SARS-CoV-2 antigens enabled orientation of antigens on the cellulose membrane and sensitive detection of SARS-CoV-2 antibodies [30,31]. CBDs were also utilized to develop nanobody-functionalized cellulose for capturing SARS-CoV-2 [32]. CBDs were demonstrated to enable the efficient orientation of capture probes (e.g., antigens and antibodies) on cellulose materials.

In the present study, we developed a colorimetric LFIA platform (a SARS-CoV-2 Ag LFIA based on a biofunctional linker CBP31-BC) for the sensitive detection of SARS-CoV-2. We probed the sensitivity and specificity of the LFIA using the SARS-CoV-2 receptor binding domain (RBD) and SARS-CoV S1 antigen. In particular, we investigated the clinical performance of the LFIA on nasopharyngeal samples from COVID-19 patients and healthy samples. Here, we report the practical feasibility of the developed LFIA platform for the sensitive detection of SARS-CoV-2.

2. Experimental section

2.1. Materials

Ampicillin, isopropyl β-D-thiogalactopyranoside (IPTG), 40-nm gold nanoparticles (AuNPs), sodium phosphate monobasic, sodium chloride, imidazole, sucrose, Tween-20, and Whatman™ Grade 1 qualitative filter paper were purchased from Sigma—Aldrich (St. Louis, MO, USA). Halt protease inhibitor cocktail (100×), 10× phosphate buffered saline (PBS), HisPur nickel-nitrilotriacetic acid (Ni-NTA) resin, and BD Difco Luria-Bertani (LB) Broth were purchased from Thermo Fisher Scientific (Waltham, MA, USA). Coomassie Brilliant Blue G-250 protein stain powder, Precision Plus Protein All Blue Prestained Protein Standards, and Protein Assay Dye Reagent Concentrate were purchased from Bio-Rad Laboratories (Hercules, CA, USA). Bovine serum albumin (BSA) and dithiothreitol (DTT) were purchased from VWR Life Science (Radnor, PA, USA) and LPS Solution (Daejeon, Korea), respectively. A 30% acrylamide-bis solution was purchased from BiOSESANG (Seongnam, Korea). SARS-CoV-2 (2019-nCoV) spike antibodies, chimeric MAb (40150-D006), SARS-CoV-2 spike neutralizing antibody, mouse MAb (40591-MM43), and SARS-CoV spike/S1 protein were purchased from Sino Biological (Wayne, PA, USA). The receptor-binding domain (RBD) of the SARS-CoV-2 spike S1 protein was purchased from HyTest (Turku, Finland). Cultured SARS-CoV-2 was purchased from ATCC (Manassas, VA, USA).

2.2. Expression and purification of the CBP31-BC protein

The recombinant CBP31-BC protein was produced in *Escherichia coli* as previously described. [26] Recombinant *E. coli* BL21 (DE3) containing pET-CBP31-BC was grown in 400 mL of LB medium (0.5 % yeast extract, 1 % tryptophan, and 1 % NaCl) with 50 μg/mL ampicillin at 37 °C. When the culture reached an optical density of ~0.8–0.9 at 600 nm (OD_{600}), 1 mM IPTG was added to induce the expression of CBP31-BC protein. The recombinant cells were incubated at 25 °C for an additional 12 h. The culture broth was then harvested by centrifugation at 4000*g* for 10 min. The cell pellets were resuspended in 5 mL of lysis buffer (50 mM NaH_2PO_4, 300 mM NaCl, and 10 mM imidazole; pH 8.0) containing 1 mM DTT and 1 mM phenylmethanesulfonyl fluoride (PMSF) per gram wet weight. The resuspended cells were disrupted using a sonic dismembrator (Qsonica, Farmingdale, NA, USA) for 10 min at 50 % power (3-sec pulse on and 2-sec pulse off). The cell lysate was centrifuged at 10, 000g for 20 min at 4 °C. The soluble fraction was then loaded onto a Ni-NTA column. The CBP31-BC protein was eluted with elution buffer (50 mM NaH_2PO_4, 300 mM NaCl, and 250 mM imidazole; pH 8.0) and dialyzed against 100 mM sodium phosphate buffer (pH 7.0). The purified CBP31-BC was stored at 4 °C until use. The Bradford assay was used to quantify the protein concentration. The protein purity was assessed using a 15 % (w/v) sodium dodecyl sulfate-polyacrylamide gel (SDS—PAGE). After electrophoresis, the gel was stained with Coomassie Blue and analyzed using Gel-Pro Analyzer software (Media Cybernetics, Silver Spring, MD).

2.3. Conjugation of AuNPs to antibodies

The SARS-CoV-2 (2019-nCoV) spike antibody (40591-MM43) was added to an AuNP solution (40 nm; suspended in 0.1 M PBS, pH 7.5) to obtain a final concentration of 10 μg/mL. The antibody solution was incubated for 1 h of incubation at 20 °C and then 2% (w/v) BSA solution (0.2 M borate buffer, pH 8.0) was added to the solution to block the nonspecific interaction of AuNP-conjugated antibodies. The resulting solution was reacted at 4 °C for an additional 2 h. The reacted solution was centrifuged at 2500*g* for 30 min at 4 °C. The pellet was collected and resuspended in 0.2 M borate buffer (pH 8.5) containing 1% (w/v) sucrose and 0.1% (w/v) BSA to increase the stability of AuNP-conjugated antibody and to minimize non-specific adsorption during the assays.

2.4. Preparation of cellulose LFIA strips

A pair of SARS-CoV-2 (2019-nCoV) spike antibodies (40591- MM43 and 40150-D006) were used with the LFIA. A SARS-CoV-2 spike antibody (40150-D006) as a capture antibody was incubated with the CBP31-BC protein for 12 h at 4 °C. CBP31-BC preincubated with the SARS-CoV-2 spike antibody and CBP31-BC alone were dispensed at the test line and control line of the cellulose membrane, respectively, at 0.05 μL/mm using an automatic dispenser. The resulting membrane was incubated for 1 h at 4 °C and cut into 3–4 mm wide strips using an automatic programmable cutter (GCI-800; Guillotine Cutting; ZETA Corporation, Gunpo, Korea). The AuNP-conjugated antibody solution was dispensed onto a conjugating pad. The sample, conjugate, and absorbent pads were pasted with a 2-mm overlap on the cellulose membrane and were then all attached to a backing card (Fig. S1). The

LFIA strip was stored in a desiccator until use.

2.5. Sensitivity and specificity analyses of the LFIA strip

SARS-CoV-2 RBD antigens and cultured SARS-CoV-2 were used to evaluate the sensitivity of the LFIA. The RBD antigen was serially diluted in running buffer (1× PBS (pH 7.4), 0.1% (v/v) Tween-20, and 2% (w/v) BSA). The final concentrations of the diluted sample ranged from 200 to 0.05 ng/mL. A total of 1×10^7 copies/mL to 1×10^4 copies/mL of a cultured SARS-CoV-2 sample were prepared by serial dilution in running buffer. PBS (1×) containing 0.1% (v/v) Tween-20 and 2% (w/v) BSA was used as a blank. A total of 120 μL of running buffer containing the RBD antigen or SARS-CoV-2 was loaded onto the sample pad. The sample was flowed through a conjugate pad, and the antibody-conjugated AuNPs recognized the antigens to form antigen-antibody complexes. The dispersion velocity of the AuNP-conjugated antibody solution was 57.6 s/4 cm, which was calculated by dividing the capillary flow time by the length of the cellulose membrane. This antigen-antibody complex was captured by the SARS-CoV-2 spike antibody with the CBP31-BC immobilized on the cellulose membrane. After 15 min of sample loading, the test and control lines turned red. The strips were photographed using a smartphone under the same conditions to minimize the effect of ambient light. After an additional process of the strip images by adjusting the brightness and contrast in the same way, the color intensities were quantified using ImageJ (NIH; Bethesda, MD, USA).

SARS-CoV S1, MERS-CoV S1, and human coronavirus (HCoV-229E) S1 were used as negative controls to validate the specificity of the LFIA for SARS-CoV-2. The antigens were prepared at three concentrations (50, 5, and 0.5 ng/mL) by diluting them in a running buffer. A 120 μL running buffer containing SARS-CoV S1, MERS-CoV S1, or HCoV-229E S1 antigens was loaded onto the sample pad. The strips were photographed using a smartphone under the same conditions to minimize the effect of ambient light. After an additional process of the strip images by adjusting the brightness and contrast in the same way, the color intensities on test and control lines were quantified using ImageJ.

2.6. Clinical performance of the LFIA strip

The clinical samples used in this study were collected from subjects using registered protocols approved by the Institutional Review Board (IRB) of the Catholic Medical Center (IRB registration number: XC21TIDI0134K). Nasopharyngeal swabs from COVID-19 patients and healthy subjects were stored in viral transport medium (VTM) (Noble Biosciences, Hwaseong, Korea). The clinical samples were inactivated by heating at 100 °C for 10 min and stored at − 80 °C for further use. All samples were tested by real-time RT—qPCR. RNA extraction from the clinical sample was performed using the QIAamp viral RNA kit (Qiagen; Hilden, NRW, Germany) by the manufacturer's manuscript. Two RdRp (IP2 & IP4) and E genes were amplified with the primers and probes (Table S1) using a superscript III platinum one-step quantitative RT—PCR kit (Thermo Fisher Scientific). The amplification was performed with 50 cycles of 95 °C for 15 s and 58 °C for 30 s on the Lightcycler 480 II real-time PCR system (Roche Diagnostics; Basel, BS, Switzerland). Nasopharyngeal swab samples from COVID-19 patients and healthy subjects were mixed with running buffer in a 1:9 (v/v) ratio and loaded onto LFIA strips. After 15 min, the strips were photographed using a smartphone under the same conditions to minimize the effect of ambient light. After an additional process of the strip images by adjusting the brightness and contrast in the same way, the color intensities on test and control lines were quantified using ImageJ.

2.7. Determination of the limit of detection

The limit of detection (LOD) of the SARS-CoV-2 RBD was calculated from a four-parameter logistic curve using a method reported by Holstein et al [33]. The variance in the mean was determined for all data points performed in replicates ($N \geq 3$) for twelve different SARS-CoV-2 RBD concentrations, including the blank, and the LOD was calculated using the following equation:

$$L_D = L_C + t[1 - \beta, m(n - 1)]\sigma_{test}$$

where σ_{test} is the pooled standard deviation of n test replicates and $t[1 - \beta, m(n - 1)]$ is the $1 - \beta$ percentile of the t distribution for $m(n - 1)$ degrees of freedom. We set both α and β to 0.05. The LOD for cultured SARS-CoV-2 was determined as the mean value of the blank plus three times the standard deviation.

2.8. Statistical methods

The Student's t test was performed to compare data from two different groups. All statistical analyses were performed using SigmaPlot ver 10.0. * $p < 0.05$, ** $p < 0.01$, and *** $p < 0.001$ were considered significant.

3. Results and discussion

3.1. Development of the CBP31-BC-based SARS-CoV-2 Ag LFIA

As the BC domains of CBP31-BC interact with any IgG molecules based on different binding affinities [34], the CBP31-BC-based LFIA is generally suitable for application to samples that do not contain antibodies. However, SARS-CoV-2-specific IgG and IgA appear in nasopharyngeal samples within 2–8 weeks after symptom onset, but not before one week after symptom onset [35,36]. Considering that a diagnosis is made early after the appearance of symptoms, we speculated that the developed LFIA could detect SARS-CoV-2 in nasopharyngeal samples without competition between the capture antibody used and other human antibodies on the BC domains. The CBP31-BC protein was produced in *Escherichia coli* as previously described [26] and purified using one-step affinity chromatography (Fig. S2). We used a chimeric monoclonal antibody with mouse variable and human kappa IgG1 constant regions as a capture antibody because BC domains strongly interact with the Fc region of human IgGs [37]. A mouse monoclonal antibody was used as the detection antibody to minimize competition between the capture and detection antibodies against CBP31-BC. The detection antibody was conjugated with AuNPs through electrostatic and physical adsorption (Fig. S3). Dot-blotting analysis was performed to determine whether the capture antibody has cross-reactivity with the detection antibody (Fig. S4). We did not observe color development of the membrane even after 1 h of incubation, indicating that the capture antibody is not cross-reactive with the detection antibody. In addition, we confirmed that the BC domains of CBP31-BC bind to the capture and detection antibodies (Fig. S5).

The CBP31-BC-based LFIA strips consisted of a sample pad, conjugate pad, cellulose membrane, and an absorbent pad (Fig. 1). The test zone of a strip was composed of CBP31-BC preincubated with an anti-SARS-CoV-2 RBD antibody (the capture antibody) at the test line and CBP31-BC alone at the control line on a cellulose membrane. Previously observed diffusion of the test and control lines was minimized by decreasing the volume of the sample loaded on the cellulose membrane [26]. To prevent nonspecific binding of CBP31-BC at the test line to the detection antibody in the absence of SARS-CoV-2 RBD, the quantity of CBP31-BC was optimized under fixed quantities of the capture antibody. A solution of CBP31-BC pre-incubated with the capture antibody at a specific ratio was dot-blotted on cellulose membrane, followed by reacting with AuNP-conjugated detection antibody in the absence of the SARS-CoV-2 RBD. The theoretical molar ratio of CBP31-BC to the capture antibody is 1 to 2. However, a test dot composed of CBP31-BC and the capture antibody in a molar ratio of 1 to 20 did not appear red when the detection antibody was added in the absence of SARS-CoV-2 RBD

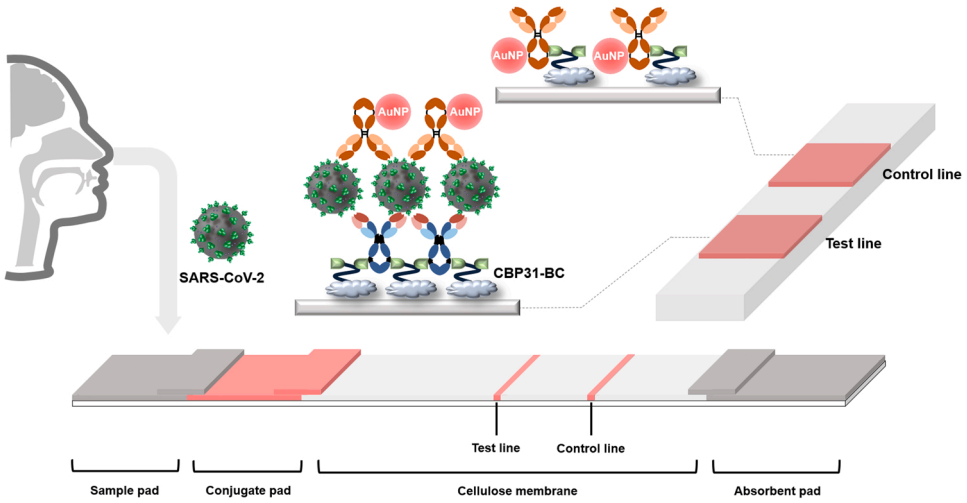

Fig. 1. Schematic of the CBP31-BC-based LFIA for the detection of SARS-CoV-2. *The LFIA strips consist* of a sample pad, conjugate pad, cellulose membrane, and absorbent pad. The test line placed on the cellulose membrane contains a capture antibody with immobilized CBP31-BC to detect the SARS-CoV-2 spike antigen. CBP31-BC alone is used for the control line. The developed LFIA can sensitively detect the SARS-CoV-2 spike antigen within 15 min.

(Fig. S6). Similarly to previously reported results [26], the experimental molar ratio might result from inaccurate quantification of the antibody and CBP3-BC. Therefore, CBP31-BC preincubated with a capture antibody in a molar ratio of 1 to 20 was applied to the test line.

3.2. Analytical performance of the CBP31-BC-based SARS-CoV-2 Ag LFIA

To evaluate the capability of the developed LFIA for detecting SARS-CoV-2, we analyzed the LFIA sensitivity using SARS-CoV-2 RBD with concentrations ranging from 0.05 to 200 ng/mL (Fig. 2). The cellulose membrane was photographed using a smartphone at 15 min after sample loading, and the color intensities of the test and control lines were analyzed. However, photographic images with weak intensities may result from inconsistencies in the surface of the cellulose paper and uneven background reflectance [38]. To overcome this problem, we are working on further studies to prepare nanocellulose membranes with even surfaces and controlled porosity using cellulose nanofibers or cellulose nanocrystals.

Each sample was assayed at least three times using the CBP31-BC-based LFIA (Fig. S7). The color intensity of the test line in the LFIA increased with the SARS-CoV-2 RBD concentration. A logistic sigmoidal calibration curve with a correlation coefficient of 0.9914 was obtained for the LFIA. A LOD of 0.63 ng/mL was calculated using a method reported in the literature [33]. This LOD was comparable with that of the SARS-CoV-2 nucleocapsid-specific LFIA based on antibody immobilization via the streptavidin-biotin interaction [39]. The relative standard deviation (RSD) in the detection results of the CBP31-BC-based LFIA was ~5 % at all SARS-CoV-2 RBD concentrations, indicating high reproducibility.

Next, the specificity of CBP31-BC-based LFIA was evaluated using the S1 antigens from coronavirus SARS-CoV, MERS-CoV, and CoV-H229E (Fig. 3). Three different concentrations (50, 5, and 0.5 ng/mL) of SARS-CoV-2 RBD, SARS-CoV S1, MERS-CoV S1, and CoV-H229E S1 were prepared and loaded onto the LFIA strips (Figs. S7 & S8). After 15 min, the intensity of the test lines was analyzed. The SARS-CoV-2 RBD was detected at a low concentration (0.5 ng/mL), whereas the SARS-CoV S1, MERS-CoV S1, and CoV-229E S1 antigens were not detected. Even at a high 50 ng/mL concentration, the SARS-CoV S1, MERS-CoV S1, and CoV-229E S1 antigens were detected at almost the same level as the blank. According to the manufacturer's information, the antibodies used in the CBP31-BC-based LFIA have cross-reactivity with the SARS-CoV S1 antigen. Thus, we speculate that the specificity

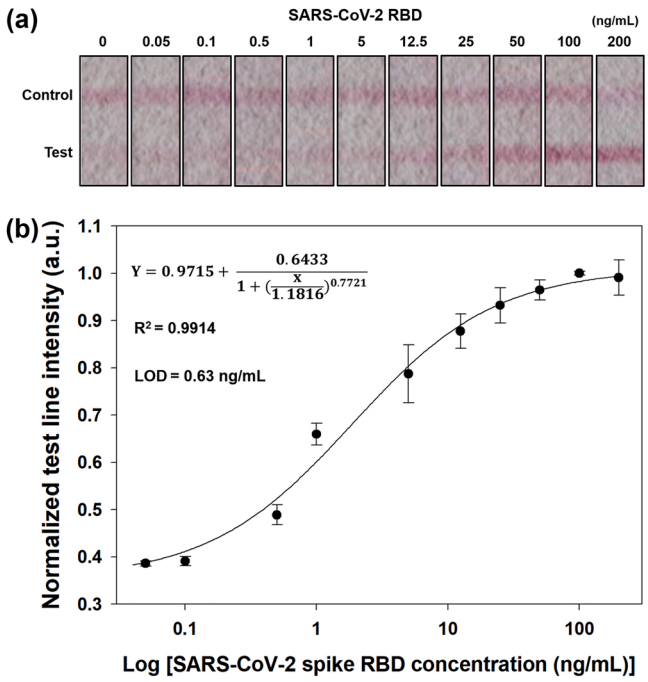

Fig. 2. Sensitivity analysis of the CBP31-BC-based LFIA. a) Photographic images showing the results of the LFIA strip for different SARS-CoV-2 RBD concentrations. The cellulose membrane was photographed using a smartphone at 15 min after sample loading, and the test line intensity was analyzed using ImageJ. b) The normalized test line intensity of the LFIA for different SARS-CoV-2 RBD concentrations. The data were fitted to a logistic four-parameter curve with a high correlation coefficient of 0.9914. All the data are presented as the mean of at least three independent measurements, and the error bars represent the standard deviation from the mean. The LOD was calculated as previously described by Holstein et al [33].

of the LFIA might result from the antibodies binding more strongly to SARS-CoV-2 RBD than to the SARS-CoV S1 antigen. Considering all the results, the developed CBP31-BC-based LFIA has high sensitivity and specificity for SARS-CoV-2 antigen detection without significant cross-reactivity with the coronavirus antigens.

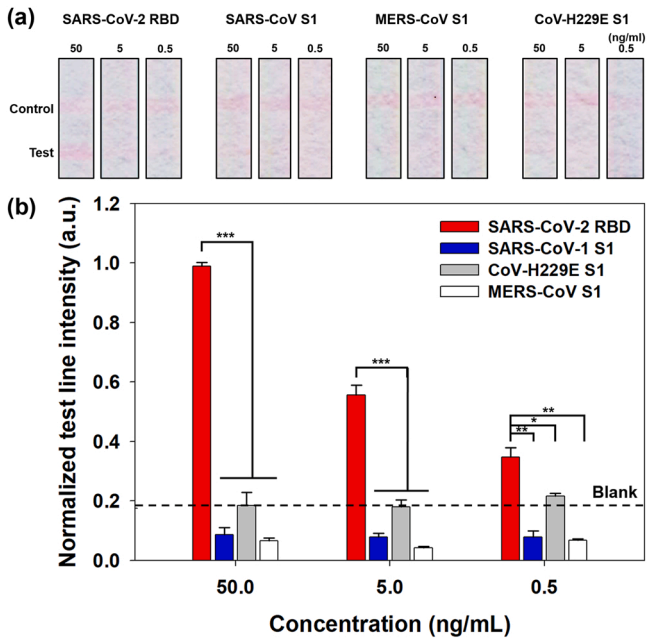

Fig. 3. Specificity analysis of the CBP31-BC-based LFIA. a) Photographic images for the cross-reactivity of the LFIA against SARS-CoV-2 RBD, SARS-CoV S1, MERS-CoV S1, and CoV-H229E S1 antigens. The cellulose membrane was photographed using a smartphone at 15 min after sample loading, and the test line intensity was analyzed using ImageJ. b) The normalized test line intensity of the LFIA for SARS-CoV-2 RBD, SARS-CoV S1, MERS-CoV S1, and CoV-H229E S1 antigens. The dotted line indicates no sample. All the data are represented as the mean of at least three independent measurements, and the error bars represent the standard deviation from the mean. P-values: *P ≤ 0.05, * *P ≤ 0.01, * **P ≤ 0.001.

3.3. Laboratory confirmation of the CBP31-BC-based LFIA using clinical samples

We evaluated the practical capability of the CBP31-BC-based LFIA using cultured SARS-CoV-2 virus samples. The cultured virus from ATCC was serially diluted from 1×10^7 copies/mL to 1×10^4 copies/mL in running buffer. The virus samples were loaded onto the LFIA strips, and the test zone was photographed using a smartphone after 15 min. Each sample was assayed at least three times using the LFIA (Fig. S9). Almost the same intensities were observed for the control lines of all the strips, when the strips were working normally. The intensity of the test line increased with the virus concentration. The visual sensitivity of the LFIA to the cultured virus was 5×10^5 copies/mL (Fig. 4a). Considering the LOD (the mean value of negative controls + 3 × standard deviation) determined by the IUPAC standard method, the CBP31-BC-based LFIA could detect SARS-CoV-2 at levels as low as 5×10^4 copies/mL (Fig. 4c), which is comparable to that of an LFIA based on a colorimetric-and-fluorescent dual signal probe [18]. The sensitivity of the developed LFIA was compared with those of previously developed LFIA strips for SARS-CoV-2 detection (Table 1).

Most rapid antigen tests for SARS-CoV-2 detect SARS-CoV-2 from the nasopharynx in an extraction buffer [7,9,14–16]. Nasopharyngeal swab samples from COVID-19 patients (n = 16) and healthy subjects (n = 3) were used for the laboratory confirmation of the CBP31-BC-based LFIA. Clinical swab samples were validated by RT—qPCR. All the clinical samples were mixed with a running buffer in a 1:9 (v/v) ratio to minimize the negative effect of the viral transport medium. Unlike the results obtained for the detection of the RBD (Fig. 2), a background signal was not detected in the test line for the cultured virus (Fig. 4a) and clinical specimens (Fig. 4b). The test and control lines in the presence of the SARS-CoV-2 virus could be observed with the naked eye. However, the band intensity of the photographic images was weak due to the inherent

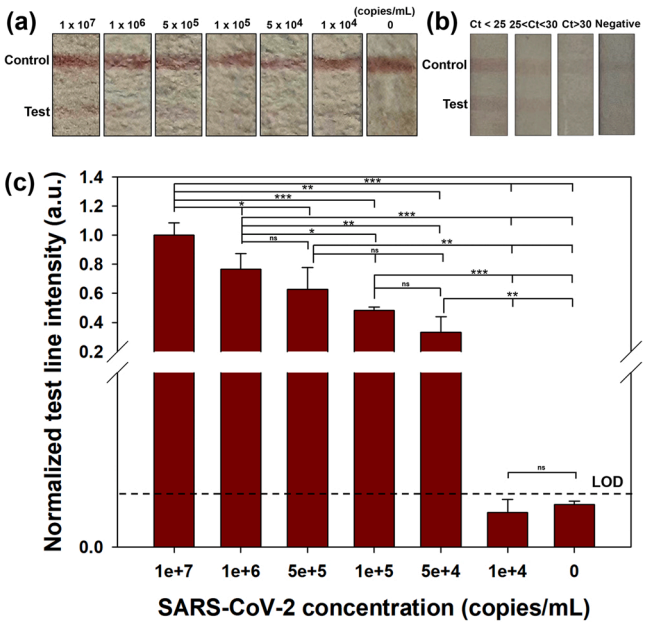

(d)

LFIA Result	PCR Result		Accuracy
	Positive	Negative	
Positive	16	0	100%
Negative	0	3	

Fig. 4. Laboratory confirmation of the CBP31-BC-based LFIA using clinical samples. a) Photographic images showing the results of the LFIA strip for different cultured SARS-CoV-2 concentrations. b) Photographic images showing the results of the LFIA strips for samples from clinical COVID-19 patients. The cellulose membrane was photographed using a smartphone at 15 min after sample loading, and the test line intensity was analyzed using ImageJ. c) The normalized test line intensity of the LFIA for different cultured SARS-CoV-2 concentrations. The black dotted line indicates the cutoff value (the mean of 3 blank samples + 3 standard deviations). All the data are represented as the mean of at least three independent measurements, and the error bars represent the standard deviation from the mean. d) Confusion matrices for evaluating the performance of the LFIA using nasophyngeal swab samples from COVID-19 patients. P-values: ns > 0.05, *P ≤ 0.05, * *P ≤ 0.01, * **P ≤ 0.001.

characteristics of the cellulose paper mentioned above. Sixteen positive results were obtained using the CBP31-BC-based LFIA for RT—qPCR-validated swab samples, and no positive signals were observed for samples from healthy subjects (Fig. 4b & 4d). Importantly, COVID-19 patient samples with low virus loads (high Ct values) were identified accurately (Fig. 4d & Table S1). The CBP31-BC-based LFIA exhibited a total accuracy of 100% for detecting SARS-CoV-2 in clinical samples. Hence, the results of the CBP31-BC-based LFIA exhibited significantly high concordance with the RT—qPCR results. Therefore, we conclude that the CBP31-BC-based LFIA is highly sensitive and accurate for the practical detection of SARS-CoV-2.

Rapid and accurate testing of SARS-CoV-2 is vital for early diagnosis and treatment to efficiently control the COVID-19 pandemic. Compared to the many LFIA platforms for SARS-CoV-2 diagnosis that have been developed, our CBP31-BC-based LFIA approach provides an alternative for accurate diagnosis using CBP31-BC-mediated oriented antibody immobilization. Compared to conventional LFIA platforms that rely on random antibody orientation by physical adsorption [40], our CBP31-BC-based LFIA platform can detect low virus loads with a Ct value above 30, resulting in a lower false-negative rate.

4. Conclusion

In this study, we developed a CBP31-BC-based LFIA platform for the

Table 1
Comparison of the analytical performance of LFIA strips for SARS-CoV-2 detection.

Ab immobilization	Signal probe	Target sample	Limit of detection	Reference
Physical adsorption	Magnetic quantum dots with triple QD shells	S1 protein NP protein	1 pg/mL 0.5 pg/mL	[20]
Physical adsorption	SiO2 @Au/QD	S1 protein Inactivated SARS-CoV-2	33 pg/mL 1.02×10^4 copies/mL	[18]
Physical adsorption	Co-Fe@heme nanocomposite	S1 protein Inactivated SARS-CoV-2	0.1 ng/mL 360 $TCID_{50}$/mL	[19]
Physical adsorption	Cellulose nanobead	NP protein Inactivated SAR-CoV-2	20 ng/mL 2.5×10^5 pfu/mL	[6]
Oriented immobilization via streptavidin-biotin interaction	AuNPs	NP protein	0.65 ng/mL	[39]
Oriented immobilization using CBP31-BC	AuNPs	RBD Inactivated SARS-CoV-2	0.63 ng/mL 5×10^4 copies/mL	This work

rapid and accurate detection of SARS-CoV-2. Our approach has the advantages of high sensitivity and specificity for SARS-CoV-2, which enables accurate detection of SARS-CoV-2 and overcomes the disadvantage of high false-negative results obtained using conventional LFIAs. Furthermore, the developed LFIA can detect low virus loads in biological media and is therefore practicable for the early diagnosis of SARS-CoV-2 in infected people. In addition, the assay did not exhibit measurable cross-reactivity with the SARS-CoV S1 antigen. Thus, the proposed method could facilitate efficient control of the COVID-19 pandemic by enabling early detection of SARS-CoV-2.

CRediT authorship contribution statement

Ae Sol Lee: Conceptualization, Methodology, Investigation, Data curation, Writing. **Su Min Kim:** Conceptualization, Methodology, Investigation, Data curation, Writing. **Kyeong Rok Kim:** Methodology, Investigation, Data curation. **Chulmin Park:** Methodology, Investigation. **Dong-Gun Lee:** Methodology, Investigation. **Hye Ryoung Heo:** Methodology, Investigation, Data curation. **Hyung Joon Cha:** Project administration, Supervision, Conceptualization, Investigation, Writing. **Chang Sup Kim:** Project administration, Funding acquisition, Supervision, Conceptualization, Investigation, Writing.

Declaration of Competing Interest

The authors declare that they have no known competing financial interests or personal relationships that could have appeared to influence the work reported in this paper.

Data Availability

Data will be made available on request.

Acknowledgements

Financial support was provided by the National Research Foundation of Korea (NRF-2019R1C1C1007379 and NRF-2022R1A5A2018865 to C. S. Kim) grant funded by the Korea government (MSIT), and the Po-Ca Networking Groups (No. 2.0080462.01 to H.J. Cha & D-G. Lee) funded by the POSTECH-Catholic Biomedical Engineering Institute (PCBMI).

Appendix A. Supporting information

Supplementary data associated with this article can be found in the online version at doi:10.1016/j.snb.2022.133245.

References

[1] N. Zhu, D.Y. Zhang, W.L. Wang, X.W. Li, B. Yang, J.D. Song, X. Zhao, B.Y. Huang, W.F. Shi, R.J. Lu, P.H. Niu, F.X. Zhan, X.J. Ma, D.Y. Wang, W.B. Xu, G.Z. Wu, G.G. F. Gao, W.J. Tan, A novel coronavirus from patients with pneumonia in China, 2019, N. Engl. J. Med. 382 (8) (2020) 727–733.
[2] W.H.O., Weekly epidemiological update on COVID-19 - 28 December 2021 (2021).
[3] F.T. Yu, L.T. Yan, N. Wang, S.Y. Yang, L.H. Wang, Y.X. Tang, G.J. Gao, S. Wang, C. J. Ma, R.M. Xie, F. Wang, C.A.R. Tan, L.X. Zhu, Y. Guo, F.J. Zhang, Quantitative detection and viral load analysis of SARS-CoV-2 in infected patients, Clin. Infect. Dis. 71 (15) (2020) 793–798.
[4] A.N. Baker, S.J. Richards, C.S. Guy, T.R. Congdon, M. Hasan, A.J. Zwetsloot, A. Gallo, J.R. Lewandowski, P.J. Stansfeld, A. Straube, M. Walker, S. Chessa, G. Pergolizzi, S. Dedola, R.A. Field, M.I. Gibson, The SARS-COV-2 spike protein binds sialic acids and enables rapid detection in a lateral flow point of care diagnostic device, ACS Cent. Sci. 6 (11) (2020) 2046–2052.
[5] C. Huang, T. Wen, F.J. Shi, X.Y. Zeng, Y.J. Jiao, Rapid detection of IgM antibodies against the SARS-CoV-2 virus via colloidal gold nanoparticle-based lateral-flow assay, ACS Omega 5 (21) (2020) 12550–12556.
[6] H.Y. Kim, J.H. Lee, M.J. Kim, S.C. Park, M. Choi, W. Lee, K.B. Ku, B.T. Kim, E. C. Park, H.G. Kim, S.I. Kim, Development of a SARS-CoV-2-specific biosensor for antigen detection using scFv-Fc fusion proteins, Biosens. Bioelectron. 175 (2021), 112868.
[7] J.H. Lee, M. Choi, Y. Jung, S.K. Lee, C.S. Lee, J. Kim, J. Kim, N.H. Kim, B.T. Kim, H. G. Kim, A novel rapid detection for SARS-CoV-2 spike 1 antigens using human angiotensin converting enzyme 2 (ACE2), Biosens. Bioelectron. 171 (2021), 112715.
[8] T. Wen, C. Huang, F.J. Shi, X.Y. Zeng, T. Lu, S.N. Ding, Y.J. Jiao, Development of a lateral flow immunoassay strip for rapid detection of IgG antibody against SARS-CoV-2 virus, Analyst 145 (15) (2020) 5345–5352.
[9] C. Zhang, T. Zheng, H. Wang, W. Chen, X. Huang, J. Liang, L. Qiu, D. Han, W. Tan, Rapid one-pot detection of SARS-CoV-2 based on a lateral flow assay in clinical samples, Anal. Chem. 93 (7) (2021) 3325–3330.
[10] M. Zou, F. Su, R. Zhang, X. Jiang, H. Xiao, X. Yan, C. Yang, X. Fan, G. Wu, Rapid point-of-care testing for SARS-CoV-2 virus nucleic acid detection by an isothermal and nonenzymatic Signal amplification system coupled with a lateral flow immunoassay strip, Sens. Actuators B Chem. 342 (2021), 129899.
[11] H.Y. Hou, T. Wang, B. Zhang, Y. Luo, L. Mao, F. Wang, S.J. Wu, Z.Y. Sun, Detection of IgM and IgG antibodies in patients with coronavirus disease 2019, Clin. Transl. Immunol. 9 (5) (2020), e1136.
[12] X. Xu, J. Sun, S. Nie, H.Y. Li, Y.Z. Kong, M. Liang, J.L. Hou, X.Z. Huang, D.F. Li, T. Ma, J.Q. Peng, S.K. Gao, Y. Shao, H. Zhu, J.Y.N. Lau, G.Y. Wang, C.B. Xie, L. Jiang, A.L. Huang, Z.L. Yang, K. Zhang, F.F. Hou, Seroprevalence of immunoglobulin M and G antibodies against SARS-CoV-2 in China, Nat. Med. 26 (8) (2020) 1193–1195.
[13] Q.X. Long, B.Z. Liu, H.J. Deng, G.C. Wu, K. Deng, Y.K. Chen, P. Liao, J.F. Qiu, Y. Lin, X.F. Cai, D.Q. Wang, Y. Hu, J.H. Ren, N. Tang, Y.Y. Xu, L.H. Yu, Z. Mo, F. Gong, X.L. Zhang, W.G. Tian, L. Hu, X.X. Zhang, J.L. Xiang, H.X. Du, H.W. Liu, C. H. Lang, X.H. Luo, S.B. Wu, X.P. Cui, Z. Zhou, M.M. Zhu, J. Wang, C.J. Xue, X.F. Li, L. Wang, Z.J. Li, K. Wang, C.C. Niu, Q.J. Yang, X.J. Tang, Y. Zhang, X.M. Liu, J. J. Li, D.C. Zhang, F. Zhang, P. Liu, J. Yuan, Q. Li, J.L. Hu, J. Chen, A.L. Huang, Antibody responses to SARS-CoV-2 in patients with COVID-19, Nat. Med. 26 (6) (2020) 845–848.
[14] F. Cerutti, E. Burdino, M.G. Milia, T. Allice, G. Gregori, B. Bruzzone, V. Ghisetti, Urgent need of rapid tests for SARS CoV-2 antigen detection: Evaluation of the SD-Biosensor antigen test for SARS-CoV-2, J. Clin. Virol. 132 (2020), 104654.
[15] L. Porte, P. Legarraga, V. Vollrath, X. Aguilera, J.M. Munita, R. Araos, G. Pizarro, P. Vial, M. Iruretagoyena, S. Dittrich, T. Weitzel, Evaluation of a novel antigen-based rapid detection test for the diagnosis of SARS-CoV-2 in respiratory samples, Int. J. Infect. Dis. 99 (2020) 328–333.
[16] A. Scohy, A. Anantharajah, M. Bodeus, B. Kabamba-Mukadi, A. Verroken, H. Rodriguez-Villalobos, Low performance of rapid antigen detection test as frontline testing for COVID-19 diagnosis, J. Clin. Virol. 129 (2020), 104455.
[17] W.H.O., Antigen-detection in the diagnosis of SARS-CoV-2 infection, (2021).
[18] H. Han, C. Wang, X. Yang, S. Zheng, X. Cheng, Z. Liu, B. Zhao, R. Xiao, Rapid field determination of SARS-CoV-2 by a colorimetric and fluorescent dual-functional lateral flow immunoassay biosensor, Sens. Actuators B Chem. 351 (2022), 130897.
[19] D. Liu, C.H. Ju, C. Han, R. Shi, X.H. Chen, D.M. Duan, J.H. Yan, X.Y. Yan, Nanozyme chemiluminescence paper test for rapid and sensitive detection of SARS-CoV-2 antigen, Biosens. Bioelectron. 173 (2021), 112817.
[20] C. Wang, X. Cheng, L. Liu, X. Zhang, X. Yang, S. Zheng, Z. Rong, S. Wang, Ultrasensitive and simultaneous detection of two specific sars-cov-2 antigens in human specimens using direct/enrichment dual-mode fluorescence lateral flow immunoassay, ACS Appl. Mater. Interfaces 13 (34) (2021) 40342–40353.
[21] C.W. Wang, X.S. Yang, S. Zheng, X.D. Cheng, R. Xiao, Q.J. Li, W.Q. Wang, X.X. Liu, S.Q. Wang, Development of an ultrasensitive fluorescent immunochromatographic assay based on multilayer quantum dot nanobead for simultaneous detection of SARS-CoV-2 antigen and influenza A virus, Sens. Actuators B Chem. 345 (2021), 130372.

[22] A. Kausaite-Minkstimiene, A. Ramanaviciene, J. Kirlyte, A. Ramanavicius, Comparative study of random and oriented antibody immobilization techniques on the binding capacity of immunosensor, Anal. Chem. 82 (15) (2010) 6401–6408.
[23] S.K. Vashist, C.K. Dixit, B.D. MacCraith, R. O'Kennedy, Effect of antibody immobilization strategies on the analytical performance of a surface plasmon resonance-based immunoassay, Analyst 136 (21) (2011) 4431–4436.
[24] S.K. Vashist, E.M. Schneider, E. Lam, S. Hrapovic, J.H.T. Luong, One-step antibody immobilization-based rapid and highly-sensitive sandwich ELISA procedure for potential in vitro diagnostics, Sci. Rep. 4 (2014) 4407.
[25] Y. Jung, J.Y. Jeong, B.H. Chung, Recent advances in immobilization methods of antibodies on solid supports, Analyst 133 (6) (2008) 697–701.
[26] J.M. Yang, K.R. Kim, S. Jeon, H.J. Cha, C.S. Kim, A sensitive paper-based lateral flow immunoassay platform using engineered cellulose-binding protein linker fused with antibody-binding domains, Sens. Actuators B Chem. 329 (2021), 129099.
[27] W. Hong, S.-G. Jeong, D.Y. Kim, S.P. Pack, C.-S. Lee, Improvement in the reproducibility of a paper-based analytical device (PAD) using stable covalent binding between proteins and cellulose paper, Biotechnol. Bioprecess Eng. 23 (2018) 686–692.
[28] X. Qin, Z. Zhang, T. Yang, L. Yuan, Y. Guo, X. Yang, Auto-fluorescence of cellulose paper with spatial solid phrase dispersion-induced fluorescence enhancement behavior for three heavy metal ions detection, Food Chem. 389 (2022), 133093.
[29] X. Qin, J. Liu, Z. Zhang, J. Li, L. Yuan, Z. Zhang, L. Chen, Microfluidic paper-based chips in rapid detection: current status, challenges, and perspectives, Trac-Trends Anal. Chem. 143 (2021), 116371.
[30] S. Kim, Y. Hao, E.A. Miller, D.M.Y. Tay, E. Yee, P. Kongsuphol, H. Jia, M. McBee, P. R. Preiser, H.D. Sikes, Vertical flow cellulose-based assays for SARS-CoV-2 antibody detection in human serum, ACS Sens 6 (5) (2021) 1891–1898.
[31] E.A. Miller, S. Baniya, D. Osorio, Y.J. Al Maalouf, H.D. Sikes, Paper-based diagnostics in the antigen-depletion regime: high-density immobilization of rcSso7d-cellulose-binding domain fusion proteins for efficient target capture, Biosens. Bioelectron. 102 (2018) 456–463.
[32] X. Sun, S. Yang, A.A. Al-Dossary, S. Broitman, Y. Ni, M. Guan, M. Yang, J. Li, Nanobody-functionalized cellulose for capturing SARS-CoV-2, Appl. Environ. Microbiol. 88 (5) (2022) e02303–e02321.
[33] C.A. Holstein, M. Griffin, J. Hong, P.D. Sampson, Statistical method for determining and comparing limits of detection of bioassays, Anal. Chem. 87 (19) (2015) 9795–9801.
[34] Y. Lee, J. Jeong, G. Lee, J.H. Moon, M.K. Lee, Covalent and oriented surface immobilization of antibody using photoactivatable antibody Fc-binding protein expressed in Escherichia coli, Anal. Chem. 88 (19) (2016) 9503–9509.
[35] B. Crescenzo-Chaigne, S. Behillil, V. Enouf, N. Escriou, S. Petres, M.N. Ungeheuer, J. Ghosn, S. Tubiana, L. Bouadma, S. van der Werf, C. Demeret, Nasopharyngeal and serological anti SARS-CoV-2 IgG/IgA responses in COVID-19 patients, J. Clin. Virol. 1 (4) (2021), 100041.
[36] F. Krempe, L. Scholer, B. Katschinski, A. Herrmann, O.E. Anastasiou, C. Elsner, R. S. Ross, F. Scholz, U. Dittmer, P. Miethe, V.T.K. Le-Trilling, M. Trilling, A rapid test recognizing mucosal SARS-CoV-2-specific antibodies distinguishes prodromal from convalescent COVID-19, Iscience 24 (10) (2021), 103194.
[37] J.B. Fishman, E.A. Berg, Protein A and protein G purification of antibodies, Cold Spring Harb. Protoc. 2019 (2019), https://doi.org/10.1101/pdb.prot099143, 2019:pdb.prot099143.
[38] T.-H. Ulep, J.-Y. Yoon, Challenges in paper-based fluorogenic optical sensing with smartphones, Nano Converg. 5 (1) (2018) 14.
[39] B.D. Grant, C.E. Anderson, J.R. Williford, L.F. Alonzo, V.A. Glukhova, D.S. Boyle, B. H. Weigl, K.P. Nichols, SARS-CoV-2 coronavirus nucleocapsid antigen-detecting half-strip lateral flow assay toward the development of point of care tests using commercially available reagents, Anal. Chem. 92 (16) (2020) 11305–11309.
[40] P.P. Down, University of Oxford SARS-CoV-2 LFD test development and validation cell. Preliminary report from the Joint PHE Porton Down & University of Oxford SARS-CoV-2 test development and validation cell: rapid evaluation of Lateral Flow Viral Antigen detection devices (LFDs) for mass community testing, 8 Novemer 2020.

Ae Sol Lee is a Ph.D. student in Biochemistry at Yeungnam University under the guidance of Prof. Chang Sup Kim. Her current research interests mainly focus on protein-based biomaterials for diagnosis and drug delivery.

Su Min Kim is an MS student in Biochemistry at Yeungnam University under the guidance of Prof. Chang Sup Kim. Her current research interests mainly focus on the development of highly sensitive lateral flow immunoassays.

Kyeong Rok Kim is a Ph.D. student in Biochemistry at Yeungnam University under the guidance of Prof. Chang Sup Kim. His current research interests focus on protein-based biomaterials for diagnosis and drug delivery.

Chulmin Park received his Ph.D. in Microbiology from Chung-Ang University in 2003. He trained post-doctoral fellowship II at Children's Hospital at Oakland Research Institutes (CHORI) in the USA from 2003 to 2005. Currently, he is a research professor at the Vaccine Bio Institute, the Catholic University of Korea. He focuses on microbial resistance, molecular epidemiology, and molecular mechanism of infection. Also, he is joining in evaluating immunity in the procedure to develop vaccines in a clinical trial.

Dong-Gun Lee received MD and Ph.D. degrees from the Catholic University of Korea and trained post-doc at the University of Wisconsin-Madison in the USA from 2006 to 2008. Currently, he is currently working as Professor at the Div. of Infectious Diseases, Dept. of Internal Medicine, College of Medicine, The Catholic University of Korea, and the Director of Transplantation & Consultation Center, Catholic Hematology Hospital, Seoul, Korea. His area of interest includes the diagnosis and management of infectious complications from hematological malignancy patients and the prevention of infectious diseases such as post-transplantation vaccination.

Hye Ryoung Heo received her Ph.D. in Interdisciplinary Bioscience & Bioengineering from Pohang University of Science and Technology (POSTECH) in 2015. She joined Yeungnam University in 2022. Currently, she is a postdoctoral researcher at Yeungnam University. Her area of interest includes biosensor-based disease diagnosis and disease-related biomarker screening.

Hyung Joon Cha received his Ph.D. in Chemical Engineering from Seoul National University in 1995. He joined Pohang University of Science and Technology (POSTECH) in 1999. Currently, he is the SeAH chair professor of POSTECH and the director of the Biomaterials Research Center. He is also the founder and Chief Technology Officer of Nature Gluetech Co., Ltd for technology commercialization of adhesive protein as an innovative medical glue. His area of interest includes structure proteins-based biomaterials, tissue, and biomedical engineering, biosensors, and biomineralization.

Chang Sup Kim received his Ph.D. in Chemical Engineering from Pohang University of Science and Technology (POSTECH) in 2013. He joined Yeungnam University in 2014. Currently, he is an associate professor at Yeungnam University. His area of interest includes biomaterial engineering for biosensors, biocatalysts, and biomedical applications.